Spring 5-11-2011

Evaluation of a Lagrangian Discrete Phase Modeling Approach for Application to Industrial Scale Bubbling Fluidized Beds

Schalk Cloete
Norwegian University of Science and Technology (NTNU), Norway

Shahriar AMini
SINTEF Materials and Chemistry, Norway

S.T. Johansen
SINTEF Materials and Chemistry

M. Braun
Ansys

B. Popoff
Ansys

EVALUATION OF A LAGRANGIAN DISCRETE PHASE MODELING APPROACH FOR APPLICATION TO INDUSTRIAL SCALE BUBBLING FLUIDIZED BEDS

S. Cloete†, S.T. Johansen†, M. Braun*, B. Popoff*, S. Amini†
† Flow Technology research group, SINTEF Materials and Chemistry,
Richard Birkelands Vei 3, 7034 Trondheim, Norway
Shahriar.Amini@sintef.no
*Ansys Germany GmbH, Birkenweg 14a, D-64295 Darmstadt, Germany

ABSTRACT
Industrial scale bubbling fluidized bed simulations were carried out within the Kinetic Theory of Granular Flows (KTGF). The KTGF was applied within two different modelling frameworks, the traditional Two Fluid Model (TFM) and a new approach in the form of the Dense Discrete Phase Model (DDPM), in order to identify any differences in performance. Only the DDPM was able to attain fully grid independent results for industrial scale 2D simulations. In fact, the performance was sufficiently good to enable the completion of reasonably affordable full 3D simulations. These simulations revealed some differences between 2D and 3D, but the global system behaviour remained relatively similar. Comparisons to experimental pressure drop data for both 2D and 3D simulations were acceptable.

INTRODUCTION
Grid independence behaviour of fluidized bed simulations depends primarily on the resolution of meso-scale particle structures in the computational domain. In bubbling beds these structures are realized as bubbles, while risers typically display the formation of particle clusters. Within industrial scale fluidized bed systems, the length scales on which these clusters occur generally requires a mesh size which is too small to be realistically simulated with present computational capacities.

In order to address this challenge, substantial research effort has been invested into filtered or 'coarse graining' approaches (1-5). These methods aim to model the effects of particle structures so that they do not have to be directly resolved on a very fine grid. The filtered approach holds great promise for industrial application and has a solid fundamental basis, but after a decade of study is still said to be in its infancy when reviewed for the highly sensitive Geldart A particle class (6). In order to arrive at a complete predictive model for industrial reactors, these closures will have to be extended to poly-dispersed particle systems and additional closures will have to be formulated for reaction kinetics. It is therefore reasoned that it will be many years before a sufficiently generic and reliable set of sub-grid closures will be developed.

The alternative to the filtered approach is fully resolving all the particle structures on a sufficiently fine computational grid. When using this approach, no modelling is needed in addition to the standard Kinetic Theory of Granular Flows (KTGF). Using the traditional Two Fluid Model (TFM), grid independent results cannot be attained for industrial reactors, but an alternative modelling formulation, known as the Dense Discrete Phase Model (DDPM), has been shown to display much improved grid independence behaviour (7). This modelling approach will now be evaluated in an industrial scale bubbling bed reactor without any sub-grid closures incorporated in order to assess the degree to which it can improve grid independence behaviour.

SIMULATIONS

Model equations

Simulations will be carried out both with the TFM and the DDPM in order to compare their grid independence behaviour. A summary of the TFM model equations for this approach can be found in Taghipour *et al.* (8). The most important closure relations employed was the modelling of the drag and solids viscosity according to Syamlal *et al.* (9), the frictional viscosity according to Schaeffer (10), the solids pressure according to Lun *et al.* (11) and the radial distribution function according to Ogawa et al. (12). The granular temperature equation was only solved in its algebraic form, thereby neglecting the contributions of convection and diffusion.

Due to its novelty, a more complete description of the DDPM will be provided here. The DDPM is based on the standard Discrete Phase Modelling (DPM) approach where parcels of particles are tracked through the domain in a Lagrangian framework according to Newton's laws of motion. In its standard form, the DPM does not account for the volume fraction of the discrete phase particles. The DDPM formulation (13) overcomes this limitation by solving a set of conservation equations for multiple phases (generalized form written below for phase *p*).

$$\frac{\partial}{\partial t}\left(\alpha_p \rho_p\right) + \nabla\left(\alpha_p \rho_p \vec{\upsilon}_p\right) = \sum_{q=1}^{n\ phases}\left(\dot{m}_{qp} - \dot{m}_{pq}\right) \qquad (1)$$

$$\frac{\partial}{\partial t}\left(\alpha_p \rho_p \vec{\upsilon}_p\right) + \nabla\left(\alpha_p \rho_p \vec{\upsilon}_p \vec{\upsilon}_p\right) = -\alpha_p \nabla p + \nabla\cdot\left[\alpha_p \mu_p\left(\nabla\vec{\upsilon}_p + \vec{\upsilon}_p^{T}\right)\right] + \alpha_p \rho_p \vec{g} + \vec{F} + \sum_{q=1}^{n\ phases}\left(K_{qp}\left(\vec{\upsilon}_q - \vec{\upsilon}_p\right) + \dot{m}_{qp}\vec{\upsilon}_{qp} - \dot{m}_{pq}\vec{\upsilon}_{pq}\right) + K_{DPM}\left(\vec{\upsilon}_{DPM} - \vec{\upsilon}_p\right) + S_{DPM,\text{explicit}} \qquad (2)$$

The conservation equations are not solved for the particulate phase, but the appropriate volume fraction or velocity values are taken directly from the particle field.

The particle equation of motion is solved for each particle in the form:

$$\frac{d\vec{\upsilon}_p}{dt} = \frac{-1}{\rho_p}\nabla p + F_D\left(\vec{\upsilon} - \vec{\upsilon}_p\right) + \frac{\vec{g}\left(\rho_p - \rho\right)}{\rho_p} + \vec{F} + \vec{F}_{\text{interaction}} \qquad (3)$$

The right hand side terms represent the pressure force, drag force, gravitational force, any additional force and the particle-particle interaction force. The drag force is calculated as in equation (4) with the drag coefficient modelled according to Syamlal *et al.* (9).

$$F_D = \frac{18\mu}{\rho_p d_p^2}\frac{C_D\,\mathrm{Re}_p}{24} \qquad (4) \qquad F_{\text{interaction}} = \frac{-1}{\alpha_p \rho_p}\nabla p_p \qquad (5)$$

The interaction force is estimated from the solids pressure gradient according to equation (5). This is a simple but fast model for the major physical effect. It does not have the highest possible accuracy but favours efficiency, in particular when compared to DEM like approaches. A major limitation of this formulation is that the particle interaction force does not contain any viscous contribution. The resistance to strain caused by the modelled shear viscosity is therefore not included. In the dense fluidized bed system simulated here, this viscous force could be of significant importance and its negligence is expected to create a more free-flowing bed than might be expected.

The granular temperature used in the KTGF is calculated in its algebraic form from the ordinary differential equation below:

$$\frac{3}{2}\left[\frac{\partial}{\partial t}\left(\alpha_p \rho_p \Theta\right)\right] = \overline{\tau}_p : \nabla \vec{v}_p + \gamma_\Theta + \phi_{pq} \qquad (6)$$

Here, the right hand side terms represent the generation of fluctuating energy by the solids stress tensor, the collisional dissipation of fluctuating energy (11) and the energy exchange between the fluctuating particles and any additional phases (14). The solids stress tensor in equation (6) is written as follows:

$$\overline{\tau}_p = -p_p \overline{I} + 2\mu_p \overline{S} + \left(\lambda_p - \frac{2}{3}\mu_p\right) \cdot \nabla \vec{v}_p \overline{I} \qquad (7)$$

Here, the solids pressure and the bulk viscosity is calculated according to Lun *et al.* (11) and the shear viscosity according to Syamlal *et al.* (9). Within these formulations, the radial distribution function is calculated according to Ogawa *et al.* (12).

Computational Domain

Simulations will be compared to pressure drop data collected from an industrial fluidized bed reactor as reported by Gobin *et al.* (15). The cylindrical reactor was 5 m in diameter and 30 m in height. It was found, however, that only 15 m of height needs to be included in the domain for the flow scenarios investigated in this study.

Both 2D and 3D simulations were conducted. The 2D simulations were carried out on a planar domain, 5 m in width and 15 m in height, while the 3D simulations were carried out in a cylindrical domain, 5 m in diameter and 15 m in height. Both domains were meshed with constant sized square (2D) or cubic (3D) structured cells according to the simulation run in question.

Material properties

The particles used in the experiments were poly-disperse with a mean diameter of 1.3 mm and a density of 850 kg/m^3, characterizing them as Geldart D particles (16). The fluidization gas was pressurized hydrocarbons with a density of 20 kg/m^3 and a dynamic viscosity of 1.5e-5 Pa.s (15).

Boundary Conditions

The bottom boundary of the domain was designated as a constant velocity inlet (0.5 m/s) to simulate a perfect plate distributor as the gas inlet. The top boundary was designated as a pressure outlet. Side boundaries were designated as walls with a

specularity coefficient of 0.01 to describe a low friction wall in the framework of the Johnson and Jackson (17) boundary condition.

Solver settings

The commercial CFD package, FLUENT 12.1 was used as the flow solver in this study. The phase-coupled SIMPLE algorithm (18) was selected for pressure-velocity coupling. All remaining equations were discretized using the QUICK scheme (19). 1st order implicit temporal discretization was used.

Operation and data extraction

Each simulation domain was initialized with a zero value for all flow variables. A region of solids at a volume fraction of 0.35 was subsequently patched into the bottom 8 m of the reactor as specified in Gobin *et al.* (15). For the DDPM, the particle parcels were injected in the first 0.1 s of the simulation from all of the internal surfaces of the mesh. This was done in such a way that the each cell in the lower 8 m of the reactor would, on average, contain 10 particle parcels.

Following the patching and injection, the simulation was run until a quasi-steady state was reached. This was identified by a monitor on the solids velocity. Once the quasi-steady state was attained, the sampling of time statistics was activated in order to get time-averaged axial pressure profiles for each simulation. Time statistics were collected for a minimum of 30 s real time which was tested to be representative of the time-averaged system behaviour.

RESULTS AND DISCUSSION

As is often the case in industrial reactors, experimental values of pressure drop can only be estimated from the available data (15). Only two pressure measurements were available in the 5 m ID reactor, one at a height of 3.5 m and the other at a height of 6.5 m. The pressure drop between them was experimentally measured to be between 9 and 11 kPa. An average of 10 kPa will be taken. Some more detailed pressure drop measurements were made in a pilot scale unit scaled to one third of the industrial one. These measurements confirmed a virtually linear pressure drop profile along the height of the pilot scale reactor. Under the assumption that the pressure drop profile in the industrial scale reactor is linear as well, a linear pressure drop of 10000/(6.5-3.5)=3333 Pa/m can be deduced. The total pressure drop over the reactor can be estimated from the weight of the solids that has to be fluidized as 23348 Pa. An estimated linear pressure profile can therefore be specified with a gradient of 3333 Pa/m and a y-intercept of 23348. Numerical simulations will be compared against this experimental estimation.

The first set of simulations was carried out in 2D on grids spanning from 4 cm to 16 cm. In the domain simulated, this translated to cell counts between 2930 and 46875. The simulation results attained with the TFM and the DDPM are given in Figure 1.

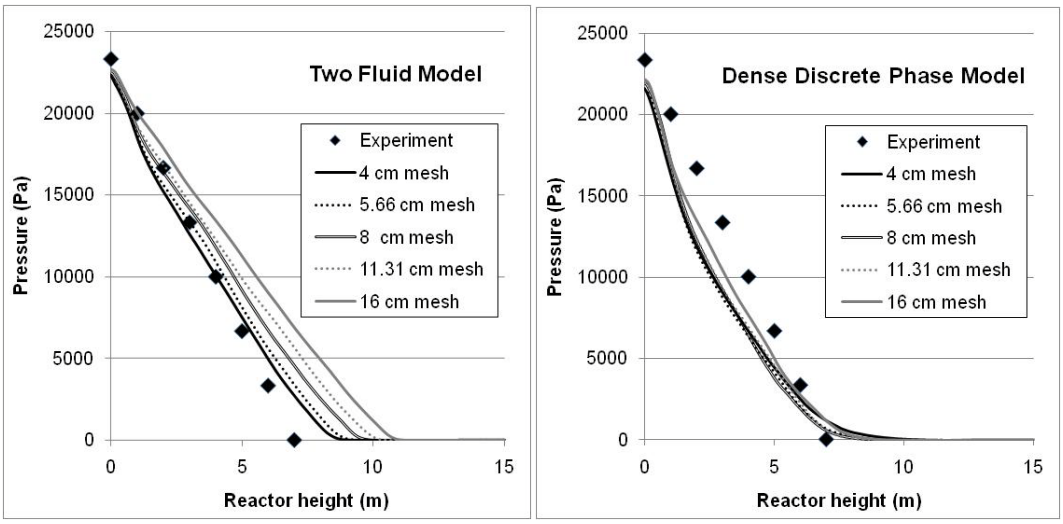

Figure 1: Pressure drop profiles for the 2D simulations with the TFM (left) and the DDPM (right) for various mesh sizes from 4 cm to 16 cm.

It is clear that both modelling approaches provide adequate fits to the estimated experimental data. The important finding for this study, however, is that the DDPM seems to retain grid independent behaviour throughout with all the grids investigated while the TFM never reaches complete grid independence. Grid independent results for the DDPM with the 16 cm grid implies that reliable results in an industrial reactor can be attained within an industrial reactor with only 2930 cells in 2D. This simulation required about 1 hour of processing time on a single processor, which, in terms of CFD standards, is very fast.

In comparison to the TFM, where grid independence might be attained on a 4 cm grid, the DDPM solved on a 16 cm grid would require 16 times less cells in 2D and can be run at a 4 times greater timestep. On a fixed grid, the DDPM is currently about 3 times slower than the TFM, but even with this taken into account, the DDPM can provide grid independent results more than 20 times faster than the TFM.

The reason for the good grid independence behaviour displayed by the DDPM is similar to the conclusions drawn in Cloete *et al.* (7) – the Lagrangian particle tracking provides for a much more accurate representation of the volume fraction field. The volume fraction field tracked by the TFM on coarse grids is subject to substantial numerical diffusion and the large volume fraction gradients cannot be resolved accurately. Instantaneous plots of the volume fraction are displayed in Figure 2 as illustration of this point.

Figure 2 shows very clear differences between the volume fraction fields resolved by the TFM and the DDPM. In the DDPM, there is a very clear separation between the bubble and emulsion phases on all the grids investigated, while the TFM does not resolve clear bubbles even on the finest grid investigated. When looking at the DDPM, it is clear that some of the flow detail is lost on the coarser grids, but Figure 1 shows that the global system behaviour is preserved, at least from a hydrodynamic point of view. The degree to which this will be true for reaction kinetic simulations is a subject for future study.

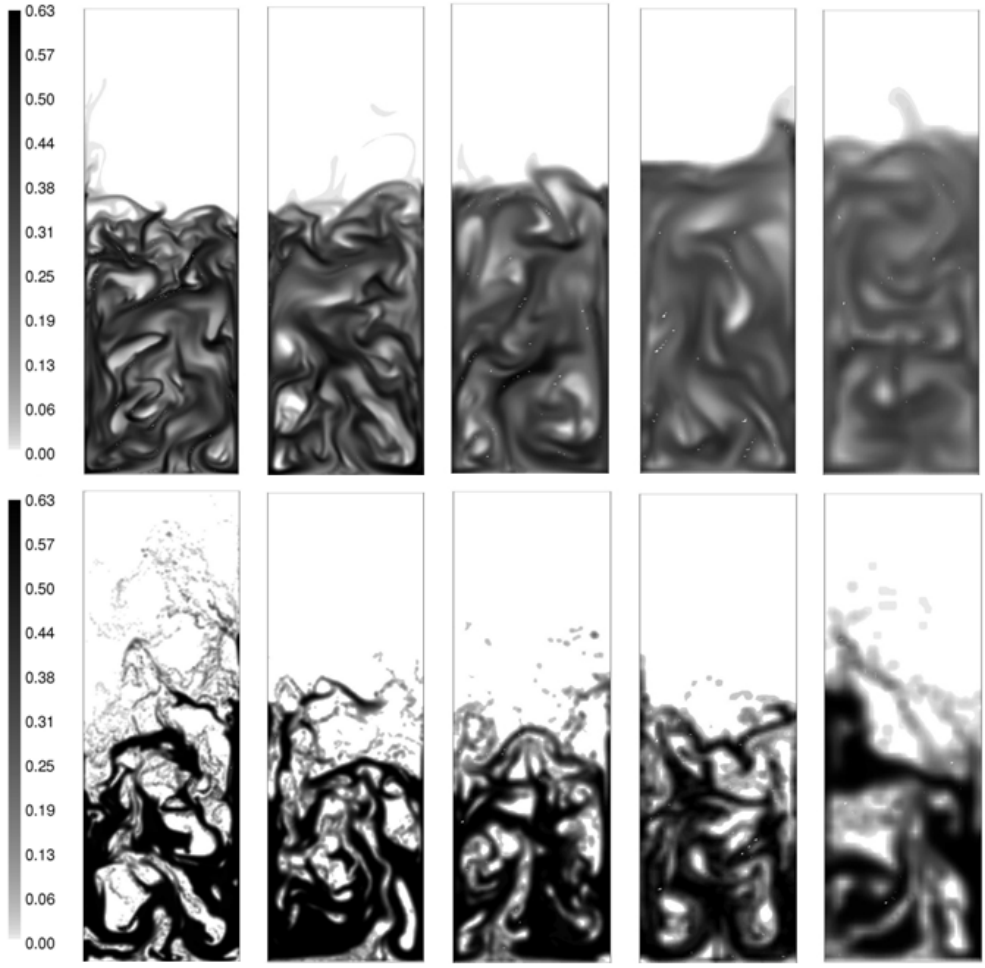

Figure 2: Instantaneous volume fraction profiles for the TFM (top) and the DDPM (bottom). The mesh is coarsened from left to right from 4 cm to 16 cm.

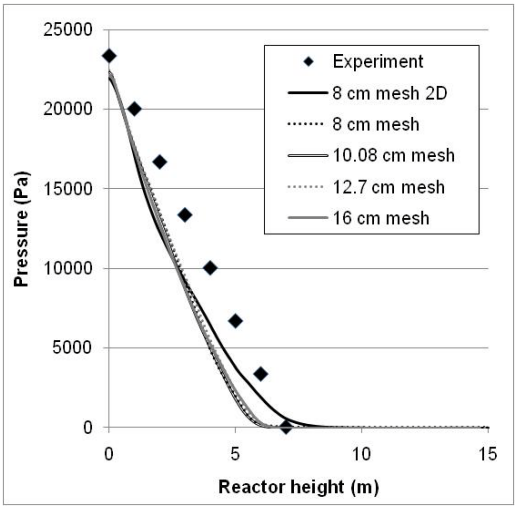

Figure 3: Pressure drop profiles for 3D simulations carried out with the DDPM for various mesh sizes from 4 cm to 16 cm.

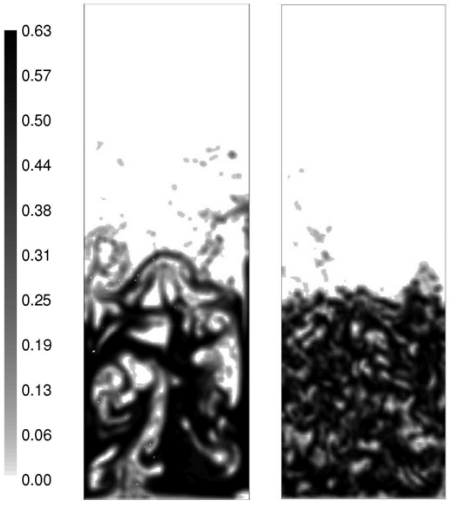

Figure 4: Comparison between the solids volume fraction profiles returned by the DDPM for the 2D and 3D cases with an 8 cm grid.

Following the good grid independence shown by the DDPM on coarse grids, some 3D simulations were also completed for grids of 8 cm and larger. The pressure profiles in Figure 3 show that the 3D simulations also display very satisfactory grid independence behaviour. Comparison to experimental data also shows acceptable agreement, even though a possible under-prediction of bed expansion is observed. In comparison to 2D simulations, the 3D runs also seem closer to reality in that they display a more linear pressure drop trend.

Figure 3 seems to indicate that 2D simulations can adequately predict global system behaviour in comparison to 3D at significantly reduced computational costs. When looking at the solids volume fraction profiles (Figure 4), however, significant differences between the 2D and 3D representations are observed. It is clear that the 3D simulations display much smaller bubbles than their 2D counterparts, especially towards the upper regions of the bed. The large voidage at the top of the 2D bed would explain the reduction in the pressure gradient towards the surface.

This pronounced difference between particle structure representation in 2D and 3D implies that 2D simulations of 3D industrial beds should be interpreted with caution. The similarity in pressure drop and bed height does suggest that the global system behaviour is preserved even in 2D, but the local transport phenomena in the bed seem to be significantly different. The system seems to be very forgiving towards these differences in terms of global hydrodynamic behaviour, but is likely to be less so when reaction kinetics are eventually incorporated.

CONCLUSIONS

Industrial scale bubbling fluidized bed simulations were carried out using the traditional Two Fluid Model (TFM) and a new approach known as the Dense Discrete Phase Model (DDPM). The DDPM showed substantially better grid independence behaviour than the TFM. 2D simulations showed that results could be attained at least 20 times faster with the DDPM than with the TFM.

Grid independence results with the DDPM were so encouraging that even reasonably affordable 3D simulations could be completed. Comparisons to experimental pressure drop data also proved to be acceptable. It was shown that differences exist between the axial pressure profiles for 2D and 3D cases, but these differences are not as large as might be expected. The local volume fraction distribution through the respective domains did show substantial differences, however, with the 2D simulations showing the formation of much larger bubbles than their 3D counterparts. These differences seem to have only a minor influence on global parameters such as pressure drop and bed height, but should be further investigated in more detailed studies.

ACKNOWLEGMENT

The authors would like to acknowledge the financial support of the Research Council of Norway under the Flow@CLC grant. Futhermore, the authors acknowledge the use of the supercomputing facilities at the Norwegian University of Science and Technology.

NOTATION

Regular symbols

C	Coefficient
d	Diameter (m)

Greek letters

α	Volume fraction
ϕ	Rate of energy exchange (W/m^3)

F	Force (1/s)	γ_Θ	Energy dissipation rate (W/m^3)
$\vec{F}$	Force vector per unit volume (N/m^3)	μ	Viscosity (Pa.s)
$\vec{g}$	Gravity vector (m/s^2)	Θ	Granular temperature (m^2/s^2)
$\overline{I}$	Identity tensor	ρ	Density (kg/m^3)
K	Interphase exchange coefficient	$\overline{\tau}$	Stress-strain tensor
$\dot{m}$	Mass transfer rate (kg/s/m^3)	$\vec{\upsilon}$	Velocity vector (m/s)
p	Pressure (Pa)	∇	Gradient (1/m)
Re	Reynolds number	*Subscripts*	
S	Source term (kg/m^{2}s^2)	D	Drag
t	Time (s)	p	Phase *p* or Particle/Solids
		q	Phase *q*
		T	Transpose

REFERENCES

1. Agrawal K, Loezos PN, Syamlal M, Sundaresan S. Journal of Fluid Mechanics. 2001;445:151-85.
2. Wang J, Ge W, Li J. Chemical Engineering Science. 2008;63(6):1553-71.
3. Igci Y, Andrews AT, Sundaresan S, Pannala S, O'Brien T. AIChE Journal. 2008;54(6):1431-48.
4. Benyahia S. Industrial and Engineering Chemistry Research. 2010;49:5122-31.
5. Andrews AT, Loezos PN, Sundaresan S. Industrial and Engineering Chemistry Research. 2005;44(16):6022-37.
6. Wang J. Industrial & Engineering Chemistry Research. 2009;48(12):5567-77.
7. Cloete S, Johansen ST, Braun M, Popoff B, Amini S. 7th International Conference on Multiphase Flow; 2010; Tampa, FL USA; 2010.
8. Taghipour F, Ellis N, Wong C. Chemical Engineering Science. 2005;60(24):6857-67.
9. Syamlal M, Rogers W, O'Brien TJ. Springfield: National Technical Information Service 1993.
10. Schaeffer DG. Journal of Differential Equations. 1987;66:19-50.
11. Lun CKK, Savage SB, Jeffrey DJ, Chepurniy N. Journal of Fluid Mechanics. 1984;140:223-56.
12. Ogawa SU, A.; Oshima, N. Journal of Applied Mathematics and Physics. 1980;31:483.
13. Popoff B, Braun M. A Lagrangian Approach to Dense Particulate Flows. *6th International Conference on Multiphase Flow*. Leipzig, Germany 2007.
14. Gidaspow D, Bezburuah R, Ding J. Hydrodynamics of Circulating Fluidized Beds, Kinetic Theory Approach. *7th Engineering Foundation Conference on Fluidization* 1992:75-82.
15. Gobin A, Neau H, Simonin O, Llinas J, Reiling V, Selo J. International journal for numerical methods in fluids. 2003;43(10-11):1199.
16. Geldart D. Powder Technology. 1973;7(5):285-92.
17. Johnson PC, Jackson R. Journal of Fluid Mechanics. 1987;176:67-93.
18. Patankar S. Hemisphere Publishing Corporation 1980.
19. Leonard BP, Mokhtari S. NASA TM 1-2568 (ICOMP-90-12); 1990; NASA Lewis Research Center; 1990.